ELECTROANALYTICAL CHEMISTRY AND INTERFACIAL ELECTROCHEMISTRY
Elsevier Sequoia S.A., Lausanne – Printed in The Netherlands

DOUBLE POTENTIAL STEP CHRONOCOULOMETRY

PART I. A REEXAMINATION OF EC KINETIC THEORY INCLUDING THE EFFECTS OF ELECTRODE REACTANT AND PRODUCT ADSORPTION

THOMAS H. RIDGWAY, RICHARD P. VAN DUYNE* AND CHARLES N. REILLEY
Department of Chemistry, University of North Carolina, Chapel Hill, N. C. 27514 (U.S.A.)
(Received 8th March 1971)

The electrode reaction sequence involving a homogeneous chemical reaction following a charge transfer step (EC mechanism)

$$A \pm ne^- \rightleftarrows B \qquad B + X \underset{k_b}{\overset{k_f}{\leftrightarrows}} Z$$

(I) (II)

in which the electrode reaction product, B, decays via (pseudo) first-order kinetics to form Z which is electrochemically inert at the potentials where reaction (I) proceeds, is frequently encountered in theoretical and experimental studies[1-22]. Recent theoretical contributions based on the integral equation method[23] and/or finite difference methods[24] have extended the theory of the EC mechanism to include reactions involving dimerization of the electrode reaction product and reaction (II) stoichiometries other than 1 : 1. Technique specific reviews are available which detail the application of a.c. methods[25], controlled potential coulometry in bulk solution[26], hydrodynamic electrodes[27], cyclic voltammetry[28], thin-layer electrochemistry[29,30], chronopotentiometry[31], and potentiostatic relaxation techniques[32] to the study of EC electrode mechanisms.

Schwarz and Shain[13] have described the chronoamperometric response for a double potential step experiment where the potential is stepped from some initial value, E_i, where no current flows to a potential, E_f, which causes the electrode reaction product, B, to be generated at a diffusion-controlled rate; after a given generation time, τ, the potential is returned to E_i where the electrode reaction is reversed consuming B at a diffusion-controlled rate. For situations exhibiting the decay kinetics of reaction II with $k_b = 0$, the current measured during the reverse step will be less than if B were stable indefinitely. It was shown that the ratio of the reverse step current measured at a time $(t-\tau)$ to the forward step current measured at a corresponding time is an effective measure of the rate of decay of B and is independent of electrode area, bulk concentration of A, and the diffusion coefficients of all species. The theory for this type of experiment was verified using the "well studied" azobenzene–$HClO_4$ system[10,11,13,37]. Double potential step chronoamperometric theory has recently been extended to include similar dimensionless current ratio expressions for dimerization[33] and disproportionation of B (ref. 34).

Christie[4] has proposed the use of double potential step chronocoulometry,

* Present address: Department of Chemistry, Northwestern University, Evanston, Illinois 60201, U.S.A.

the integrated response analog of the experiment described by Shain, for the study of EC and catalytic following reactions. Although no experimental work has appeared in the literature to substantiate the chronocoulometric theory for EC reactions, the catalytic regeneration of Ti(IV) from electrogenerated Ti(III) by hydroxylamine has been studied and the catalytic theory verified[44]. In analogy with the chronoamperometric experiment, the ratio of the charge passed in the reverse potential step to that accumulated in the forward potential step is the dimensionless kinetic parameter of interest in chronocoulometry having the characteristic value 0.5858 in the absence of all complicating factors. The principal advantage of the chronocoulometric approach is that the Q–t response can be corrected for non-diffusional contributions such as double layer charging and adsorption.

The work to be presented here results from an attempt to generate the numerical data, $|Q_b/Q_f|$ *vs.* $(k\tau)^{\frac{1}{2}}$, corresponding to Fig. 3 of ref. 4, by a slightly modified version of Feldberg's digital simulation technique. The validity of the computer program written to carry out the finite difference calculations[35] was established by simulating the known solutions to the diffusion problems for the simple reversible electron transfer and the EC mechanism for the electroanalytical techniques: (1) cyclic voltammetry, (2) single and double potential step chronoamperometry, and (3) double potential step chronocoulometry. In all cases except that of the EC mechanism in double potential step chronocoulometry, the agreement between simulated results and previously published analytical results was excellent. In order to resolve this one apparent discrepancy, the analytical solution to the chronocoulometry EC kinetics problem was rederived. The charge ratios, $|Q_b/Q_f|$, calculated from this new analytical solution were now in agreement with those calculated by the finite difference method.

Experimental verification of the newly derived working curve, $|Q_b/Q_f|$ *vs.* $(k\tau)^{\frac{1}{2}}$, was attempted using systems of current interest, namely the reductions of *p*-iodonitrobenzene[36] and 2-nitropropane[20]. Both attempts lead to inconclusive results due to complications caused by the transfer of more than $1e^-$ in the forward potential step. Subsequently the azobenzene–hydrazobenzene system, which undergoes the benzidine rearrangement in acid solution, was chosen for this study since: (*i*) its EC mechanism is well established, (*ii*) the half-life of the following reaction can be conveniently varied by changing the pH of the solution, and (*iii*) extensive kinetic data are available for comparison. Adsorption, however, is a seriously complicating factor. From previous studies, the electrode reactant, azobenzene, is known to adsorb substantially[12,13,37] and indirect evidence is available suggesting that the electrode product hydrazobenzene is adsorbed as well[11,37]. In contrast to the chronoamperometric study of Schwarz and Shain, where the adsorption contributions to the measured response could be neglected since the anomalous adsorption current component decayed much faster than the desired faradaic current, the present chronocoulometric work must explicitly account for the effects of electrode reactant and product adsorption since the integral readout "memorizes" the adsorption transient. The details of the azobenzene experimental work are given in the accompanying paper[47].

Treatments have recently appeared in the literature for dealing with the problem of the combined coupling of electroactive species adsorption and chemical reactions to the heterogeneous electron-transfer process for cyclic voltammetry[37], polarography[38], and a.c. impedance methods[39,40]. In addition, Koopman has presented a very elegant theoretical and experimental investigation of the reaction scheme:

$$\begin{array}{ccccc} A_{ads} & \overset{e^-}{\leftrightarrows} & B_{ads} & \xrightarrow{k_{het}} & C_{ads} \xrightarrow{z_1 e^-} D_{ads} \\ \Updownarrow & & \Updownarrow & & \Updownarrow \\ A_{soln} & & B_{soln} & & D_{soln} \end{array} \qquad \text{(III)}$$

as studied by double potential step chronocoulometry[41]. The reduction of nitrobenzene in aqueous alkaline buffers at an HMDE was used to test salient features of the theory. The step potentials for the double step excitation signal were selected such that the formation and disappearance of A_{ads} and B_{ads} proceeded at a diffusion limited rate. Linear adsorption isotherms were postulated to relate the bulk and surface concentrations of the electroactive species. Neglecting the second electron transfer, the reaction scheme treated by Koopman is the surface reaction analog of the homogeneous solution-reaction sequence necessary to describe, at least to a first approximation, the reduction of azobenzene in acidic solutions. Although conceptually similar, the surface-reaction scheme and the homogeneous reaction scheme lead to quantitative differences in the reverse step $Q-t$ response. We have, therefore, solved the electrochemical diffusion problem for double potential step chronocoulometry involving both EC kinetics and adsorption of the electrode reactant and product:

$$\begin{array}{ccccc} A_{ads} & \overset{e^-}{\leftrightarrows} & B_{ads} & & \\ \Updownarrow & & \Updownarrow & \overset{k_1}{} & \\ A_{soln} & & B_{soln} & \xrightarrow{} & Z_{soln} \end{array}$$

From this treatment, a relatively simple procedure has been developed which permits correction of the experimentally determined charge ratios for the effects of adsorption and double-layer charging.

COMPARISON OF ANALYTICAL SOLUTION AND FINITE DIFFERENCE SOLUTION RESULTS FOR IRREVERSIBLE EC MECHANISM — NO ADSORPTION

The rederivation of the analytical expression employed Shain's solution to the boundary value problem[13] followed by integration in the transform plane to obtain the charge. The final expression for $Q_b(t>\tau)$ is:

$$Q_b(t>\tau) = \frac{2nFAD_A^{\frac{1}{2}}C_A^*}{\pi^{\frac{1}{2}}}\left[t^{\frac{1}{2}} - \{(t-\tau)^{\frac{1}{2}}\}\Xi(k_1, t, \tau)\right] \qquad \text{(1a)}$$

where

$$\Xi(k_1, t, \tau) = e^{-k_1 t}\sum_{j=0}^{\infty}\frac{[k_1(t-\tau)]^j\,{}_1F_1(j+\frac{1}{2}, j+1, k_1\tau)\,{}_1F_1(1, j+\frac{3}{2}, k_1(t-\tau)]}{j!(2j+1)} \qquad \text{(1b)}$$

Numerical values of $|Q_b/Q_f|$ computed using eqn. (1) were in agreement with values computed using eqns. 39 and 40 of ref. 4 confirming the correctness of Christie's derivation.

$|Q_b/Q_f|$ values were also calculated by the explicit finite difference technique with 300 time increments in both the forward and reverse steps. It is a necessary condition that the stability parameter[42] used in this finite difference scheme be $\leqslant \frac{1}{2}$ for a stable, convergent solution to exist; however, this is not a sufficient condition. For

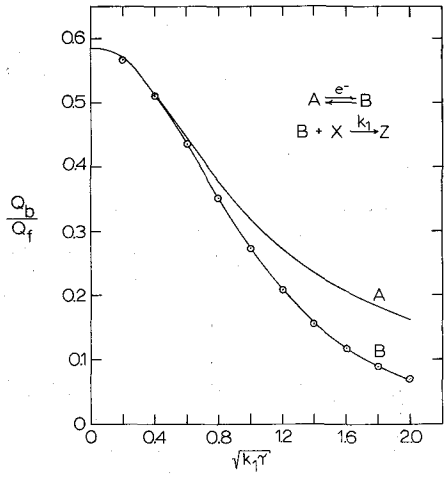

Fig. 1. Double potential step chronocoulometry working curves, $|Q_b/Q_f|$ *vs.* $(k_1\tau)^{\frac{1}{2}}$, for a first-order following reaction (EC mechanism). (A) Measured from photographic enlargement of Fig. 3 of ref. 4. (B) Calculated using eqn. (1); ⊙, Points calculated by explicit finite difference simulation—300 time increments.

TABLE 1

DIMENSIONLESS CHARGE RATIO Q_b/Q_f FOR DOUBLE POTENTIAL STEP CHRONOCOULOMETRY. COMPARISON OF SOLUTIONS FOR IRREVERSIBLE (PSEUDO)FIRST-ORDER SUCCEEDING REACTION

$(k_1\tau)^{\frac{1}{2}}$	*Christie*[a]	*Analytical*[b]	*Finite difference*
0.00	0.5858	0.5858	0.5857
0.10	0.5838	0.5808	
0.20	0.5706	0.5662	0.5656
0.30	0.5473	0.5429	
0.40	0.5157	0.5123	0.5116
0.50	0.4824	0.4761	
0.60	0.4463	0.4363	0.4354
0.70	0.4131	0.3947	
0.80	0.3800	0.3530	0.3519
0.90	0.3470	0.3126	
1.00	0.3190	0.2746	0.2734
1.10	0.2927	0.2398	
1.20	0.2716	0.2085	0.2072
1.30	0.2542	0.1809	
1.40	0.2376	0.1569	0.1554
1.50	0.2230	0.1362	
1.60	0.2096	0.1186	0.1172
1.70	0.1958	0.1037	
1.80	0.1832	0.0911	0.0897
1.90	0.1715	0.0805	
2.00	0.1613	0.0716	0.0701

[a] Measured from photographic enlargement of Fig. 3, ref. 4. [b] Computed using eqn. (1).

these calculations, the stability parameter was fixed at the value $\frac{1}{6}$, which minimizes the truncation error. That no significant change in the value of the $|Q_b/Q_f|$ ratio at several different values of $(k_1\tau)^{\frac{1}{2}}$ was observed when the number of time increments

was increased to 1000 or 2000 was taken as an indication that the solution had converged.

Figure 1 summarizes the relevant results and Table 1 provides a numerical comparison.

EC kinetics with electrode reactant and product adsorption

If, in addition to an irreversible first-order follow up reaction, the heterogeneous charge process is complicated by electrode reactant and product adsorption, the dependence of the charge ratio, $|Q_b/Q_f|$, on the kinetic parameter $(k_1\tau)^{\frac{1}{2}}$ will no longer exhibit the relatively simple behavior depicted in Fig. 1. The effects of adsorption on the Q ratio have been considered in terms of the equilibrium adsorption–EC kinetics model:

$$A_{ads} \rightleftharpoons A_{soln} \tag{IV}$$

$$A_{soln} \pm ne^- \rightleftharpoons B_{soln} \tag{V}$$

$$B_{soln} + X_{soln} \xrightarrow{k_1} Z_{soln} \tag{VI}$$

$$B_{soln} \rightleftharpoons B_{ads} \tag{VII}$$

The boundary value problem corresponding to this reaction sequence for the double potential step chronocoulometric experiment is a composite of the non-adsorption problem considered in the previous section and the adsorption case treated previously by Anson and coworkers[43]. The assumptions used by Anson (namely: (1) A reacts electrochemically at a diffusion-controlled rate following the forward potential step and B likewise following the reverse potential step; (2) an adsorbed substance reacts immediately when the potential is stepped; (3) double-layer charging is essentially instantaneous compared to τ) are considered to apply to reactions (IV)–(VII). In addition, it is assumed that: (a) no heterogeneous surface reaction of B_{ads} occurs, (b) Z and X are not adsorbed, (c) the surface excess of B, Γ_B, is less than that of A, and (d) adsorption equilibrium is attained sufficiently rapidly that Γ_A and Γ_B are independent of the switching time.

The mass-transfer equations given by Shain[13] remain valid for reaction sequence (IV)–(VII); however, the initial and boundary conditions must be restated to include adsorption contributions:

$$C_A(x, 0) = C_A^*;\ C_B(x, 0) = 0 \tag{2}$$

$$\Gamma_A(0) = \Gamma_A^*;\ \Gamma_B(0) = 0 \tag{3}$$

$$C_A(x \to \infty, t) = C_A^*;\ C_B(x \to \infty, t) = 0$$

$$C_A(0, t \leqslant \tau) = 0;\ \Gamma_A(t \leqslant \tau) = 0 \tag{4}$$

$$C_B(0, t > \tau) = 0;\ \Gamma_B(t > \tau) = 0 \tag{5}$$

$$\frac{i}{nFA} = D_A \left.\frac{\partial C_A(x, t)}{\partial x}\right|_{x=0} \tag{6a}$$

$$-\frac{\partial \Gamma_A(t)}{\partial t} = -D_B \left.\frac{\partial C_B(x, t)}{\partial x}\right|_{x=0} + \frac{\partial \Gamma_B(t)}{\partial t} \tag{6b}$$

where Γ_A^* is the initial adsorbed surface concentration of A. The charge consumed during the chronocoulometric experiment is related to the surface concentrations and fluxes in the Laplace plane by transforming eqn. (6) and multiplying by s^{-1}. The result in terms of the electrode product species, B, is:

$$\frac{\bar{Q}(s)}{nFA} = -\frac{D_B}{s}\left[\frac{d\bar{C}_B(x,s)}{dx}\bigg|_{x=0}\right] + \overline{\Gamma_B(s)} - \frac{\Gamma_B(0)}{s} \tag{7}$$

Calculating the surface flux transform of B for the two time segments of the double potential step using Shain's procedure[13] and combining with the appropriate boundary condition transforms, eqns. (4) and (5), we obtain for $t \leqslant \tau$:

$$\frac{\bar{Q}(s)}{nFA} = \frac{D_A^{\frac{1}{2}} C_A^*}{s^{\frac{3}{2}}} + \frac{\Gamma_A^*}{s} \tag{8}$$

and for $t > \tau$:

$$\frac{\bar{Q}(s)}{nFA} = D_A^{\frac{1}{2}} C_A^* \sum_{j=0}^{\infty} \left[\frac{\Gamma(j+\frac{1}{2}) k_1^j (1 - e^{-(s+k_1)\tau}\, {}_1F_1(j+\frac{1}{2}, j+1, k_1\tau))}{\pi^{\frac{1}{2}} j!\, s(s+k_1)^{j+\frac{1}{2}}}\right] + (\Gamma_A^* - \Gamma_B)\left[\frac{\operatorname{erf}\{(s+k_1)\tau\}^{\frac{1}{2}}}{s}\right] \tag{9}$$

The Q–t behavior follows immediately from the inverse Laplace transform of eqns. (8, 9)

$$Q_f(t \leqslant \tau) = 2nFAD_A^{\frac{1}{2}} C_A^* \left(\frac{t}{\pi}\right)^{\frac{1}{2}} + nFA\Gamma_A^* + Q_{dl} \tag{10}$$

$$Q_b = \frac{2nFAD_A^{\frac{1}{2}} C_A^*}{\pi^{\frac{1}{2}}}\left[t^{\frac{1}{2}} - \{t-\tau\}^{\frac{1}{2}} \Xi(k_1, t, \tau)\right] + \frac{2nFA(\Gamma_A^* - \Gamma_B)}{\pi} e^{-k_1 t}\left[\sin^{-1}(\tau/t)^{\frac{1}{2}} + 2\int_0^{(k_1\tau)^{\frac{1}{2}}} \frac{y^2\, {}_1F_1(1, \frac{3}{2}, y^2)\,dy}{(k_1 t - y^2)^{\frac{1}{2}}}\right] \tag{11}$$

where Q_{dl} is the charge consumed by the double layer charging process, y is a dummy integration variable, and $\Xi(k_1, t, \tau)$ is given by eqn. (1b). A more complete derivation of these equations has been given elsewhere[48].

The charge ratio, $|Q_b/Q_f|$, is formulated from eqn. (10) evaluated at $t=\tau$ and eqn. (11) at $t=2\tau$. The result is:

$$\left|\frac{Q_b}{Q_f}\right| = \frac{[1 - 2^{\frac{1}{2}} + \Xi(k_1\tau, 2\tau)] - Q_I + Q_{II}}{1 + Q_{II}} \tag{12}$$

where

$$Q_I = \frac{nFA(\Gamma_A^* - \Gamma_B)}{2Q_c} e^{-2k_1\tau}\left[1 + \frac{8}{\pi} G(k_1\tau, 2\tau)\right] \tag{13}$$

$$G(k_1\tau, 2\tau) = \int_0^{(k_1\tau)^{\frac{1}{2}}} \frac{y^2\, {}_1F_1(1, \frac{3}{2}, y^2)\,dy}{(2k_1\tau - y^2)^{\frac{1}{2}}} \tag{14}$$

$$Q_{II} = \frac{nFA\Gamma_A^* + Q_{dl}}{Q_c} \tag{15}$$

and Q_c is the Cottrell charge passed during the forward potential step.

$$Q_c = 2nFAD_A^{\frac{1}{2}}C_A^* \left(\frac{\tau}{\pi}\right)^{\frac{1}{2}} \tag{16}$$

The physical significance of the terms Q_I and Q_{II} is readily recognized. Q_{II} is the nondiffusing charge component which immediately appears in the $Q(t \leqslant \tau)$ transient following application of the forward potential step. Q_I, on the other hand, represents a diffusing charge component which describes the participation of solution phase B, generated at $t=0$ from originally adsorbed A, in the following chemical reaction (V). It is apparent from eqn. (12) that the magnitudes of Q_I and Q_{II} are controlled by the amount of charge contributed by adsorbed material *relative* to the diffusion only charge Q_c rather than by the absolute value of the adsorbed charge.

The effects of adsorption on the $|Q_b/Q_f|$ ratio as a function of τ are more readily apparent if the τ dependence in eqn. (12) is made explicit and the nondiffusing charges $nFA\Gamma_B$ and Q_{dl} are expressed relative to $nFA\Gamma_A$. The appropriate definitions are

$$\beta\tau^{-\frac{1}{2}} = \frac{nFA\Gamma_A^*}{Q_c} = \frac{\pi^{\frac{1}{2}}\Gamma_A^*}{2D_A^{\frac{1}{2}}C_A^*}\tau^{-\frac{1}{2}} \qquad 0 \leqslant \beta\tau^{-\frac{1}{2}} \leqslant 0.1 \tag{17}$$

$$\phi = \Gamma_B/\Gamma_A^* \qquad 0 \leqslant \phi \leqslant 1 \tag{18}$$

$$\gamma = nFA\Gamma_A^*/Q_{dl} \qquad 0 < \gamma \leqslant 1 \tag{19}$$

where the ranges of $\beta\tau^{-\frac{1}{2}}$ and γ are arbitrarily imposed, but correspond to realistic experimental situations. The range of ϕ follows from the assumption that $\Gamma_B \leqslant \Gamma_A^*$. Reformulating eqns. (12–15) in terms of the above definitions gives:

$$\left|\frac{Q_b}{Q_f}\right| = \frac{[1-2^{\frac{1}{2}}+\Xi(k_1\tau, 2\tau)]+\beta\tau^{-\frac{1}{2}}[(1+\gamma^{-1})-(1-\phi)H(k_1\tau, 2\tau)]}{1+\beta\tau^{-\frac{1}{2}}(1+\gamma^{-1})} \tag{20a}$$

where

$$H(k_1\tau, 2\tau) = \tfrac{1}{2}e^{-2k_1\tau}\left[1+\frac{8}{\pi}G(k_1\tau, 2\tau)\right] \tag{20b}$$

Values of $H(k_1\tau, 2\tau)$ were obtained by numerical integration of eqn. (14). Identical results were obtained using both Simpson's rule and gaussian quadrature integration methods. The H function is plotted as a function of the kinetic parameter $(k_1\tau)^{\frac{1}{2}}$ in Fig. 2.

In contrast to the $|Q_b/Q_f|$ expression derived for the nonadsorption EC kinetic case where one parameter, $(k_1\tau)^{\frac{1}{2}}$, served to characterize the behavior of the charge ratio, the more general expression, eqn. (20), requires independent specification of k_1, τ, the adsorption parameters β and ϕ, and the double layer charging parameter γ. As a result no one working curve analogous to Fig. 1 can be constructed which adequately describes the effects of these quantities on $|Q_b/Q_f|$. Graphical presentation of the theoretical results, therefore, consists of a series of plots $|Q_b/Q_f|$ *vs.* $\log(\tau^{\frac{1}{2}})$ for representative values of a given parameter with all others held constant. In order to simplify presentation and facilitate comparison of adsorption-kinetic controlled $|Q_b/Q_f|$ values with the simple diffusion controlled value 0.5858, Q_{dl} will be neglected, *i.e.* $\gamma^{-1}=0$. The actual practice of determining a rate constant from experimental data, however, requires consideration of double layer charging contributions.

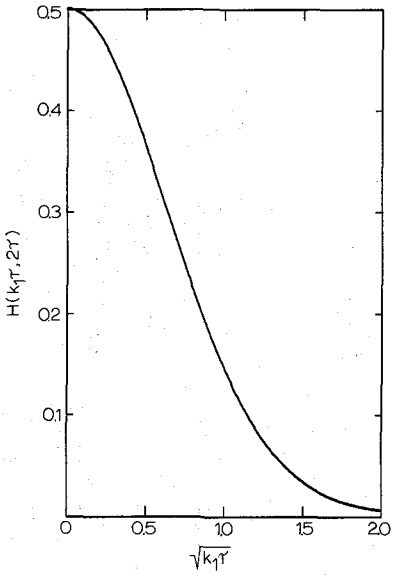

Fig. 2. Kinetic function, $H(k_1\tau, 2\tau)$ *vs.* $(k_1\tau)^{\frac{1}{2}}$ for solution-phase electrode reaction product species generated from initially adsorbed reactant. EC mechanism with adsorption of reactant and product.

Effect of adsorption on Q_b/Q_f in the absence of chemical kinetics

Anson[43] has shown that electrode reactant and product surface excesses can be determined from the intercepts of the plots $Q_f(t \leqslant \tau)$ *vs.* $t^{\frac{1}{2}}$ and $Q_r(t > \tau)$ *vs.* θ where $Q_f(t \leqslant \tau)$ is given by eqn. (10) in this work and $Q_r(t > \tau)$ is

$$Q_r(t>\tau) = \frac{2nFAD_A^{\frac{1}{2}}C_A^*}{\pi^{\frac{1}{2}}}\theta + nFA(\Gamma_A^* - \Gamma_B)\left[1 - \frac{2}{\pi}\sin^{-1}\left(\frac{\tau}{t}\right)^{\frac{1}{2}}\right] + nFA\Gamma_B + Q_{dl} \quad (21)$$

$$\theta = (t-\tau)^{\frac{1}{2}} + \tau^{\frac{1}{2}} - t^{\frac{1}{2}}$$

When the reverse step Q–t expression, eqn. (11), is subtracted from eqn. (10) evaluated at $t=\tau$ and the limit taken as $k_1 \to 0$, our results reduce identically to Anson's eqn. 29. The surface excesses were given by

$$\frac{{}^{\circ}Q_f - {}^{\circ}Q_r}{1-a_0} = nFA(\Gamma_A^* - \Gamma_B) \quad (22)$$

$$\frac{{}^{\circ}Q_r - a_0\,{}^{\circ}Q_f}{1-a_0} = nFA\Gamma_B + Q_{dl} \quad (23)$$

${}^{\circ}Q_f$ and ${}^{\circ}Q_r$ are the intercepts of the $Q_f(t \leqslant \tau)$ *vs.* $t^{\frac{1}{2}}$ and Q_r *vs.* θ plots respectively and a_0 results from the approximation

$$\left[1 - \frac{2}{\pi}\sin^{-1}\left(\frac{\tau}{t}\right)^{\frac{1}{2}}\right] \approx \frac{a_1\theta}{\tau^{\frac{1}{2}}} + a_0 \quad (24)$$

The effects of reactant and product adsorption on the value of the $|Q_b/Q_f|$ ratio were not, however, explicitly given although the analogous effect of Q_{dl} was briefly considered by Christie and Lingane[44]. An understanding of how adsorption affects $|Q_b/Q_f|$

in the non-kinetic case is useful since it will be encountered: (i) in the short time ($\tau \rightarrow 0$) limit of the kinetic case and (ii) in studies of pseudo first-order following reactions where removal of a reactant is feasible.

Taking the appropriate limits,

$$\lim_{k_1 \rightarrow 0} \Xi(k_1\tau, 2\tau) = 1 \quad \text{and} \quad \lim_{k_1 \rightarrow 0} H(k_1\tau, 2\tau) = \tfrac{1}{2},$$

eqn. (20) reduces to

$$\left|\frac{Q_b}{Q_f}\right| = \frac{(2-2^{\frac{1}{2}}) + \frac{1}{2}\beta\tau^{-\frac{1}{2}}(1+\phi)}{1+\beta\tau^{-\frac{1}{2}}} \tag{25}$$

Plots of the charge ratio against $\log(\tau^{\frac{1}{2}})$ for various values of the species A adsorption parameter, β, at constant values of the surface excess ratio, ϕ, are given in Figs. 3.1–3.3. The values of β were selected to cover the range 0 to 0.10 $s^{\frac{1}{2}}$. This is equivalent to a variation in Γ_A^* of 0 to 3.56×10^{-10} mol cm^{-2} for a solution with $C_A^* = 1 \times 10^{-3} M$ and $D_A = 10^{-5}$ cm^2 s^{-1}.

The principal influence adsorption has on the charge ratio is the introduction of a strong reversal time, τ, dependence. This is in contrast to the diffusion controlled case where $|Q_b/Q_f|$ has the constant value 0.5858 independent of τ (strictly true only when Q_{dl} contribution is neglected). Positive deviations from the diffusional value are observed for the case of equal reactant and product adsorption ($\phi = 1$) while negative deviations are observed in the reactant only adsorption case ($\phi = 0$). As is found with other electrochemical methods which study adsorption in competition with diffusional processes, the deviations of $|Q_b/Q_f|$ from the diffusion-controlled response are most significant at short measurement times and/or small bulk electroactive species concentration, *i.e.* large β. The positive and negative Q ratio deviations are consequences of the charge partitioning process during the reverse step portion of the double potential step experiment. The fraction of charge passed in the forward step due to adsorbed A, $nF\,A\Gamma_A^*$, is divided into a non-diffusing component, $nF\,A\Gamma_B$, and a diffusing component, $nFA(\Gamma_A^* - \Gamma_B)$. Under conditions where reactant and product are equally adsorbed, all the forward step adsorption charge is converted into non-diffusion $nFA\Gamma_B$. In the case of reactant adsorption only, however, the forward step adsorption charge is completely converted into diffusing charge. Diffusional losses prevent complete recovery of $nFA(\Gamma_A^* - \Gamma_B)$ coulombs from the diffusing component during the reverse step, whereas all the charge of the non-diffusing component is recovered. Therefore, when $nFA(\Gamma_A^* - \Gamma_B)$ is maximized (minimized) at $\phi = 0$ ($\phi = 1$), the charge recovered during the reverse step is minimized (maximized), and correspondingly the charge ratio, $|Q_b/Q_f|$, is minimized (maximized). In fact, setting eqn. (25) equal to $2-2^{\frac{1}{2}}$, the diffusion controlled value, and solving for ϕ, one finds that for values of $\phi > 3-2\cdot2^{\frac{1}{2}}$ the charge ratio will exceed the diffusional value while for $\phi < 3-2\cdot2^{\frac{1}{2}}$ it will be less. For ϕ exactly equal to $(3-2\cdot2^{\frac{1}{2}})$, diffusional charge losses on the reverse potential step will be balanced by adsorption charge recovery and $|Q_b/Q_f|$ will be independent of τ and have the diffusion controlled value. The charge ratio behavior for an intermediate ratio of adsorbed product to adsorbed reactant ($\phi = 0.5$) for various values of β is given in Fig. (3.3) and the effect of varying ϕ at constant $\beta = 0.050$ is shown in Fig. (3.4).

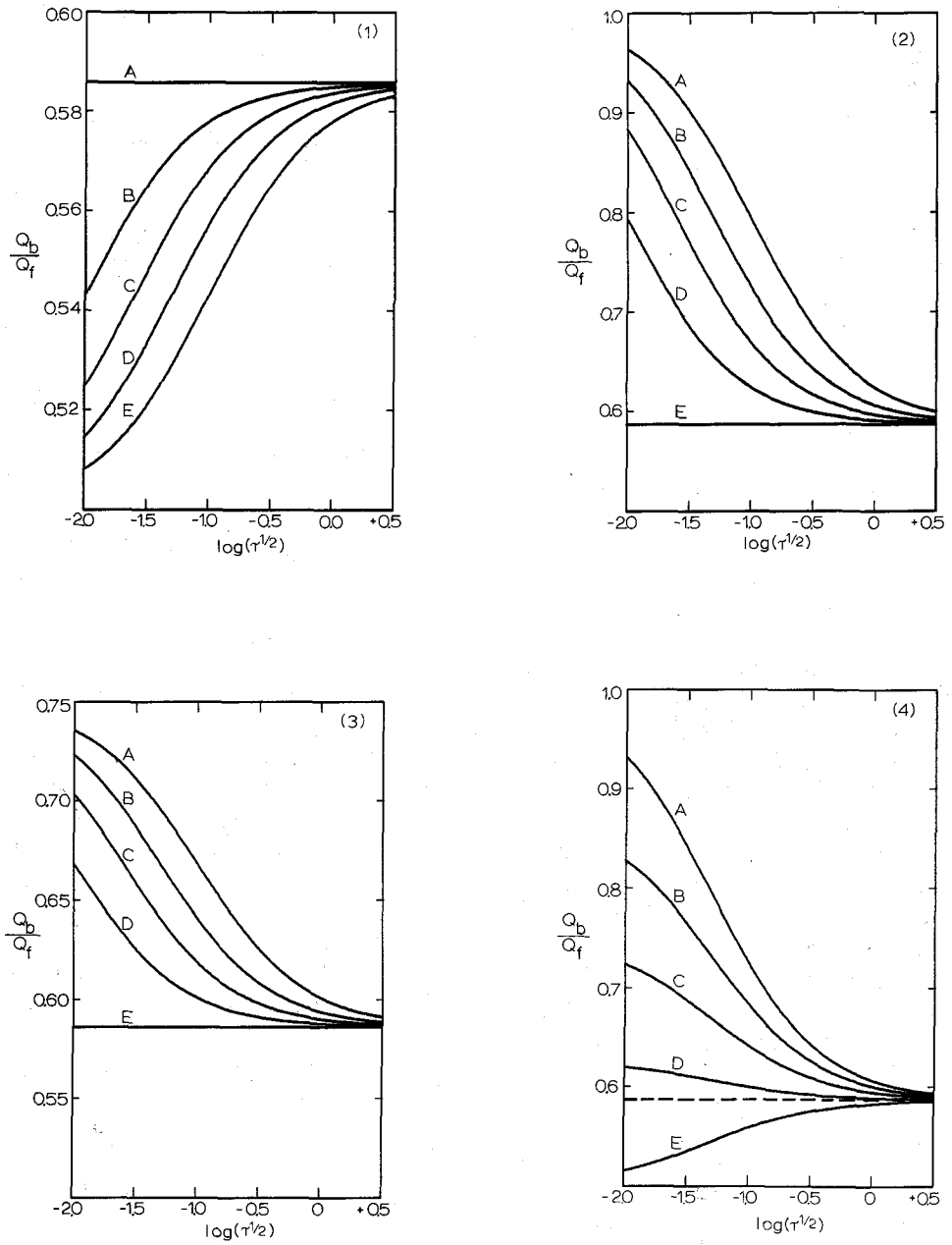

Fig. 3. The effect of reactant and product surface excesses on the double potential step chronocoulometry dimensionless charge ratio, $|Q_b/Q_f|$, *vs.* $\log(\tau^{\frac{1}{2}})$ in the absence of chemical kinetics ($k_1 = 0.0\ s^{-1}$; $\gamma^{-1} = 0$). (1) Effect of reactant surface excess. No product adsorption. $\phi = 0$; β values: A 0.00, B 0.01, C 0.025, D 0.050, E 0.10 $s^{\frac{1}{2}}$. (2) Effect of reactant surface excess. Equal adsorption of reactant and product. $\phi = 1.0$; β values: A 0.10, B 0.05, C 0.025, D 0.01, E 0.00 $s^{\frac{1}{2}}$. (3) Effect of reactant surface excess. Reactant surface excess greater than product surface excess. $\phi = 0.50$; β values: A 0.10, B 0.05, C 0.025, D 0.01, E 0.00 $s^{\frac{1}{2}}$. (4) Effect of product reactant surface excess ratio. $\beta = 0.05\ s^{\frac{1}{2}}$; ϕ: A 1.0, B 0.75, C 0.50, D 0.25, E 0.00; (------) Diffusion-controlled value 0.5858 occurs at $\phi = 3 - 2\sqrt{2}$.

Combined effects of EC kinetics and adsorption on $|Q_b/Q_f|$

In the absence of adsorption, $|Q_b/Q_f|$ decreases monotonically from the diffusion controlled value 0.5858 to 0 as the rate of the following chemical reaction increases (Fig. 1). Simultaneous consideration of adsorption and chemical kinetics is expected to result in a superposition of the individual kinetic and adsorption behaviors. Typical results illustrating the variation of the $|Q_b/Q_f|$ *vs.* $\log(\tau^{\frac{1}{2}})$ curve with changes in the chemical reaction rate constant are shown in Fig. 4. The adsorption

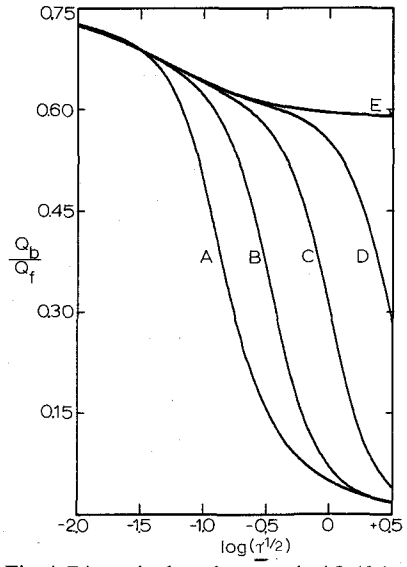

Fig. 4. Dimensionless charge ratio, $|Q_b/Q_f|$, *vs.* $\log(\tau^{\frac{1}{2}})$. Effect of the following chemical reaction rate constant. $\phi=0.5$; $\beta=0.05\ s^{\frac{1}{2}}$; $\gamma^{-1}=0$; k_1: A 10^2, B 10^1, C 1, D 10^{-1}, E 0 s^{-1}.

parameters β and ϕ have been fixed at the midpoints of their ranges. In the short time limit where the chemical reaction does not consume an appreciable quantity of species B during the time available for reaction, 2τ, the kinetic curves A–D merge with the adsorption controlled curve E. As the switching time is increased, the relative contribution of adsorption decreases and the effects of the chemical reaction predominate. The adsorption effect is, however, residual in chronocoulometry and at sufficiently long times eqn. (25) reduces to

$$\left|\frac{Q_b}{Q_f}\right| = \frac{\beta\tau^{-\frac{1}{2}}}{1+\beta\tau^{-\frac{1}{2}}} \tag{26}$$

The long time limit of the Q ratio, therefore, is characterized by a $\tau^{-\frac{1}{2}}$ approach to zero. Except for $k_1 > 100\ s^{-1}$ this long time adsorption controlled behavior will be difficult to observe experimentally due to onset of convective mass transport. Eqn. (26) accounts for the long time merger of curves A and B in Fig. 4.

The behavior of the charge ratio at a constant but non-zero value of the chemical reaction rate constant for various values of the adsorption parameters is illustrated in Figs. 5.1–5.4. The limiting cases of reactant adsorption only ($\phi=0$) and equal adsorption of reactant and product ($\phi=1$) are considered in Figs. 5.1 and 5.2, re-

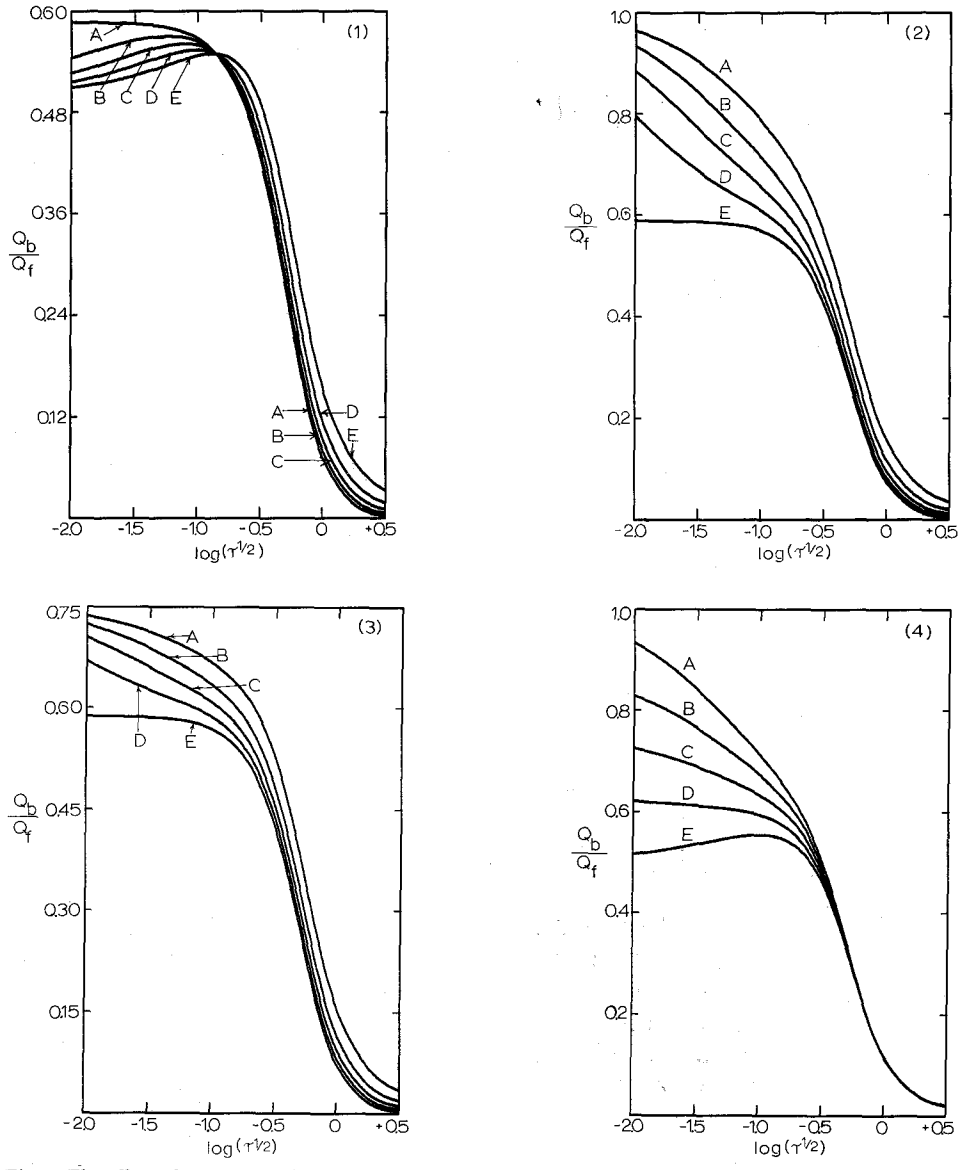

Fig. 5. The effect of reactant and product surface excesses on the double potential step chronocoulometry dimensionless charge ratio, $|Q_b/Q_f|$, *vs.* $\log(\tau^{\frac{1}{2}})$ with chemical kinetic complications ($k_1 = 4.0\ s^{-1}$; $\gamma^{-1} = 0$). (1) Effect of reactant surface excess. No product adsorption. $\phi = 0$; β values: A 0.00, B 0.01, C 0.025, D 0.05, E 0.10 $s^{\frac{1}{2}}$. (2) Effect of reactant surface excess. Equal adsorption of reactant and product. $\phi = 1.0$; β values: A 0.10, B 0.05, C 0.025, D 0.01, E 0.00 $s^{\frac{1}{2}}$. (3) Effect of reactant surface excess. Reactant surface excess greater than product surface excess. $\phi = 0.50$; β values: A 0.10, B 0.05, C 0.025, D 0.01, E 0.00 $s^{\frac{1}{2}}$. (4) Effect of product reactant surface excess ratio. $\beta = 0.05\ s^{\frac{1}{2}}$; ϕ: A 1.0, B 0.75, C 0.50, D 0.25, E 0.0.

spectively. The effect of varying ϕ at constant β is shown in Fig. 5.4. In all cases the results can be qualitatively interpreted in terms of a superposition of adsorption and kinetic effects.

Determination of the chemical reaction rate constant

The foregoing theoretical analysis has shown that for adsorption complicated EC kinetics, the double potential step chronocoulometry charge ratio is a function of two adsorption parameters and a double-layer charging parameter as well as the following chemical reaction rate constant. Extraction of k_1 from the adsorption complicated Q–t response can be effected in a relatively simple manner by correcting experimentally determined $|Q_b/Q_f|$ for the effects of adsorption and double layer charging. The expression for the adsorption corrected charge ratio, $|Q_b/Q_f|_{cor}$, is obtained by solving either eqn. (12) or eqn. (20) for the quantity $(1-\sqrt{2+\Xi(k_1\tau, 2\tau)})$, which is the EC working curve expression in the absence of adsorption and double layer complications, and using eqns. (22, 23) to substitute the experimental observables, ${}^{\circ}Q_f$ and ${}^{\circ}Q_r$, for the surface excesses and Q_{dl}. The result is:

$$\left|\frac{Q_b}{Q_f}\right|_{cor} = [1-2^{\frac{1}{2}}+\Xi(k_1\tau, 2\tau)]$$

$$= \left| \frac{(Q_r^E(2\tau)-{}^{\circ}Q_f) + \left(\frac{{}^{\circ}Q_f-{}^{\circ}Q_r}{1-a_0}\right) H(k_1\tau, 2\tau)}{Q_f^E(\tau)-{}^{\circ}Q_f} \right| \qquad (27)$$

where the superscript E denotes an experimental measurement uncorrected for adsorption. The utilization of eqn. (27) involves two readily apparent difficulties: (*i*) the following chemical reaction causes a time-dependence change in the reverse step Q_r–t transient such that a plot of Q_r *vs.* θ is no longer linear. This precludes determination of ${}^{\circ}Q_r$; and (*ii*) evaluation of $H(k_1\tau, 2\tau)$ presupposes a knowledge of a value for the rate constant, k_1.

The problem associated with measuring ${}^{\circ}Q_r$ from a kinetically influenced Q–t curve can be circumvented if experimental conditions exist which permit a separation of adsorption and kinetic effects. Two such circumstances are conceivable: (1) the chemical reaction is pseudo first-order in species X (reaction VI) and removal of X to provide a $k_1=0$ condition does not alter the surface excesses of the adsorbed species; and (2) the chemical reaction is sufficiently slow that experimentally accessible τ exist where the Q–t response is essentially free of kinetic influence, $(k_1\tau)^{\frac{1}{2}} \leqslant 0.2$, and adsorption equilibrium is reestablished during the reverse potential step in a time short with respect to τ. Both of these methods result in linear Q_r *vs.* θ plots allowing ${}^{\circ}Q_r$ to be measured. Measurement of ${}^{\circ}Q_r$ at short τ, however, places a severe restriction on the maximum k_1 that can be determined using this approach. The minimum τ that can be employed is probably on the order of 0.010 s based on estimates for the time it takes to reestablish adsorption equilibrium of $\sim$0.001 s (ref. 45). Thus for $\tau_{min} \approx 0.010$ s and $(k_1\tau)^{\frac{1}{2}} \leqslant 0.2$, $k_{1_{max}} \approx 4\ s^{-1}$.

Since $H(k_1\tau, 2\tau)$ cannot be evaluated directly without first knowing k_1, the charge ratio correction must be carried out in an iterative fashion. In the first iteration, $H(k_1\tau, 2\tau)$ is set equal to its $k_1=0$ value, *i.e.* $H(0, 2\tau)=0.50$. From the $|Q_b/Q_f|_{cor.}$ calculated in the first iteration, a rate constant is obtained using an appropriate EC working curve such as Curve B of Fig. 1. This value of the rate constant is used to evaluate $H(k_1\tau, 2\tau)$ from Fig. 2 for use in the second iteration. This procedure is repeated until the change in k_1 on successive iterations is negligible with respect to the experimental error in $Q_f^E(\tau)$ and $Q_r^E(2\tau)$.

Although this iterative calculation is somewhat tedious to carry out by hand, it is readily adaptable to computerized operation through use of power series expansions for $H(k_1\tau, 2\tau)$

$$H(k_1\tau, 2\tau) = \begin{cases} (1-a_0)\left[\sum_{i=0}^{6} b_i(k_1\tau)^i\right], & 0 \leqslant k_1\tau < 1.2 \\ (1-a_0)\left[\sum_{j=0}^{4} C_j(k_1\tau)^j\right], & 1.2 \leqslant k_1\tau \leqslant 4.0 \end{cases} \tag{28}$$

and for the inverted form of the EC working curve

$$k_1\tau = \begin{cases} \sum_{i=0}^{\infty} d_i[\Xi(k_1\tau, 2\tau)]^i, & 0 < \Xi(k_1\tau, 2\tau) \leqslant 0.370 \\ \sum_{j=0}^{\infty} e_j[\Xi(k_1\tau, 2\tau)]^j, & 0.370 < \Xi \leqslant 0.5858 \end{cases} \tag{29}$$

where the power series coefficients are listed in Table 2. Eqns. (28) and (29) were obtained by a least-squares polynomial fit to the numerical representations of the appropriate equations. The power series reproduce the original numerical values to 4 significant figures over the ranges indicated.

TABLE 2

COEFFICIENTS OF THE POWER SERIES REPRESENTATIONS FOR $H(k_1\tau, 2\tau)$ AND THE INVERSE OF $\Xi(k_1\tau, 2\tau)$

i or j	$H(k_1\tau, 2\tau)$		*Inverse of* $\Xi(k_1\tau, 2\tau)$	
	b_i	c_j	d_i	e_j
0	0.467829	0.981457	4.135099	1.123768
1	−0.001594	−1.523312	−2.124115	−1.864823
2	−0.572784	0.881168	5.348707	1.722782
3	−0.124715	−0.222230	−8.125437	−9.233115
4	0.726532	0.0201681	6.684943	2.831048
5	−0.446065	—	−2.297450	−4.607925
6	0.086389	—	—	3.083944

ACKNOWLEDGEMENTS

The authors would like to thank Dr. Richard P. Buck for valuable discussions concerning certain mathematical aspects of this work. One of the authors (R.P.V.D.) wishes to acknowledge the financial support of a National Aeronautical and Space Administration fellowship (1967–1970). This work was sponsored by the UNC Materials Research Center under Contract DAHC15 67 C 0223 with the Advanced Research Projects Agency and by the Air Force Office of Scientific Research (AFOSR), USAF, under Grant AF-AFOSR-69-1625.

SUMMARY

Calculation of the theoretical double potential step chronocoulometry working curve ($|Q_b/Q_f|$ *vs.* $(k\tau)^{\frac{1}{2}}$) for an irreversible pseudo first-order chemical reaction coupled to a heterogeneous charge transfer process (EC mechanism) by finite difference methods revealed an error in the previously published working curve for this situation. The analytical solution to the mass transport equations for the EC mechanism with double potential step boundary conditions is rederived. The working curve, calculated from this new analytical solution, was in close agreement with the finite difference results.

In addition, a theoretical treatment is presented for double potential step chronocoulometry where the effect of electrode reactant and product adsorption on the charge ratio, $|Q_b/Q_f|$, both with and without EC kinetic complications, is incorporated. A procedure whereby experimentally determined charge ratios can be corrected for the effects of reactant and product adsorption has been developed.

REFERENCES

1 T. G. McCord, H. L. Hung and D. E. Smith, *J. Electroanal. Chem.*, 21 (1969) 5 and references therein.
2 M. Sluyters-Rehbach and J. H. Sluyters, *J. Electroanal. Chem.*, 26 (1970) 237.
3 T. E. Neal, *Ph. D. Thesis*, University of North Carolina, Chapel Hill, 1970.
4 J. H. Christie, *J. Electroanal. Chem.*, 13 (1967) 79.
5 J. W. Ashley and C. N. Reilley, *J. Electroanal. Chem.*, 10 (1965) 253.
6 R. I. Gelb, *Ph. D. Thesis*, University of Wisconsin, Mad., 1967.
7 T. G. McCord and D. E. Smith, *Anal. Chem.*, 42 (1970) 2.
8 W. J. Albery and S. Bruckenstein, *Trans. Faraday Soc.*, 62 (1966) 1946.
9 C. R. Christensen and F. C. Anson, *Anal. Chem.*, 36 (1964) 495.
10 B. McDuffie, L. B. Anderson and C. N. Reilley, *Anal. Chem.*, 38 (1966) 883.
11 D. M. Oglesby, J. D. Johnson and C. N. Reilley, *Anal. Chem.*, 38 (1966) 385.
12 W. M. Schwarz and I. Shain, *J. Phys. Chem.*, 70 (1966) 845.
13 W. M. Schwarz and I. Shain, *J. Phys. Chem.*, 69 (1965) 30.
14 G. Grant and T. Kuwana, *J. Electroanal. Chem.*, 24 (1970) 11.
15 W. J. Albery, M. L. Hitchman and J. Ulstrup, *Trans. Faraday Soc.*, 64 (1968) 2831.
16 H. E. Stapelfeldt and S. P. Perone, *Anal. Chem.*, 40 (1968) 815.
17 H. E. Stapelfeldt and S. P. Perone, *Anal. Chem.*, 41 (1969) 623, 628.
18 D. G. Davis and D. J. Orleron, *Anal. Chem.*, 38 (1966) 179.
19 J. R. Kuempel and W. B. Schaap, *Inorg. Chem.*, 7 (1968) 2435.
20 R. H. Gibson and J. C. Grosthwaite, *J. Amer. Chem. Soc.*, 90 (1968) 7373.
21 R. Koopman and H. Gerischer, *Ber. Bunsenges. Phys. Chem.*, 70 (1966) 127.
22 B. K. Hosvepian and I. Shain, *J. Electroanal. Chem.*, 14 (1967) 1.
23 M. S. Shuman, *Anal. Chem.*, 42 (1970) 521.
24 M. L. Olmstead, R. G. Hamilton and R. S. Nicholson, *Anal. Chem.*, 41 (1969) 260.
25 D. E. Smith, in A. J. Bard (Ed.), *Electroanalytical Chemistry, Vol. 1*, Marcel Dekker, New York, 1966, pp. 1–155.
26 A. J. Bard and K. S. V. Santhanam, in A. J. Bard (Ed.), *Electroanalytical Chemistry, Vol. 4*, Marcel Dekker, New York, 1970, pp. 215–315.
27 K. B. Prater, *Ph. D. Thesis*, University of Texas, Austin, 1970.
28 R. S. Nicholson and I. Shain, *Anal. Chem.*, 36 (1964) 706.
29 C. N. Reilley, *Rev. Pure Appl. Chem.*, 18 (1968) 137.
30 A. T. Hubbard and F. C. Anson, in A. J. Bard (Ed.), *Electroanalytical Chemistry, Vol. 4*, Marcel Dekker, New York, 1970, pp. 129–214.
31 D. G. Davis, in A. J. Bard (Ed.), *Electroanalytical Chemistry, Vol. 1*, Marcel Dekker, New York, 1966, pp. 157–196.

32 R. W. MURRAY, in A. WEISSBERGER AND B. ROSSITER (Eds.), *Techniques of Organic Chemistry*, Interscience, New York, in press.
33 M. L. OLMSTEAD AND R. S. NICHOLSON, *Anal. Chem.*, 41 (1969) 851.
34 G. KISSEL AND S. W. FELDBERG, *J. Phys. Chem.*, 73 (1969) 3082.
35 T. H. RIDGWAY, *Ph. D. Thesis*, University of North Carolina, Chapel Hill, 1971.
36 J. G. LAWLESS AND M. D. HAWLEY, *J. Electroanal. Chem.*, 21 (1969) 365.
37 R. H. WOPSCHALL AND I. SHAIN, *Anal. Chem.*, 39 (1967) 535.
38 R. I. GELB, *J. Electroanal. Chem.*, 19 (1968) 215.
39 M. SLUYTERS-REHBACH AND J. H. SLUYTERS, *J. Electroanal. Chem.*, 23 (1969) 457.
40 R. D. ARMSTRONG, *J. Electroanal. Chem.*, 22 (1969) 49.
41 R. KOOPMAN, *Ber. Bunsenges. Phys. Chem.*, 72 (1968) 32.
42 S. W. FELDBERG, in A. J. BARD (Ed.), *Electroanalytical Chemistry, Vol. 3*, Marcel Dekker, New York, 1969, p. 205.
43 F. C. ANSON, J. H. CHRISTIE AND R. A. OSTERYOUNG, *J. Electroanal. Chem.*, 13 (1967) 236.
44 P. J. LINGANE AND J. H. CHRISTIE, *J. Electroanal. Chem.*, 13 (1967) 227.
45 F. C. ANSON, J. H. CHRISTIE AND R. A. OSTERYOUNG, *J. Electroanal. Chem.*, 13 (1967) 343.
46 W. H. REINMUTH, *Anal. Chem.*, 40 (1968) 185R.
47 R. P. VAN DUYNE, T. H. RIDGWAY AND C. N. REILLEY, *J. Electroanal. Chem.*, 34 (1971) 283.
48 R. P. VAN DUYNE, *Ph. D. Thesis*, University of North Carolina, Chapel Hill, 1970.